

Spectral Tests of Models for Accretion Disks Around Black Holes

By JULIAN H. KROLIK¹

¹Department of Physics and Astronomy, Johns Hopkins University, Baltimore MD 21218, USA

1. Introduction: the Zeroth Order Picture

To test our ideas about the dynamics of accretion disks around black holes, we compare the radiation we receive from them with the radiative output predicted by our models. Standard models predict a very simple spectrum—a quasi-thermal continuum. However, even the most cursory glance at real accretion disks immediately reveals that, while there often is a spectral component resembling the expected quasi-thermal one, substantial energy is also released in quite different ways—in hard X-rays from “coronal” gas, and also in extremely non-thermal radiation from relativistic jets. In this review I will not discuss how the energy is diverted into coronæ and more strongly non-thermal channels, or how well our models for the radiation from these structures matches what is seen; the *ad hoc* elements are so strong in these models that matching them to observations does not provide strong tests of accretion disk dynamics. Instead, I will concentrate on spectral properties of the quasi-thermal continuum. Here the character of the emergent radiation is directly tied to the structure of the disk, and can in principle provide strong diagnostics of how this structure is dynamically regulated.

It is best to begin with the simplest picture: a quiescent, smooth, geometrically thin disk that is in local thermodynamic equilibrium everywhere from the marginally stable radius out to its outermost boundary. Most of the accretion energy is released at radii near $\sim 10GM/c^2$ (the radius of maximum dissipation is somewhat greater than the marginally stable radius because relativistic effects and the outward transport of energy associated with the angular momentum flux reduce the deposition of heat in the innermost part of the disk). The characteristic temperature at which this energy is radiated is then

$$T_* \sim 2 \times 10^7 \dot{m}^{1/4} m^{-1/4} \text{K}, \quad (1.1)$$

where \dot{m} is the accretion rate relative to the rate which would produce an Eddington luminosity, and m is the mass of the black hole in solar units. Thus, we expect stellar black holes to radiate primarily soft X-rays, while galactic scale black holes (as in active galactic nuclei) should radiate primarily in the ultra-violet.

This description of the spectrum can be easily refined by integrating over the actual distribution of disk dissipation. Assuming LTE, the temperature falls towards larger radius r as $r^{-3/4}$. The sum of all the local black bodies then gives an overall luminosity per unit frequency

$$L_\nu \propto \nu^{1/3} \exp(-h\nu/kT_*), \quad (1.2)$$

where the characteristic temperature T_* is approximated by the estimate of equation 1.1 (a more careful calculation would be more punctilious about the exact location of the maximum dissipation rate).

The approximate expression given in equation 1.2 can be easily compared with real spectra to gain a sense of perspective about how well our expectations are vindicated in real objects. Ironically, the quality of data at our disposal is much better for AGN than for Galactic black holes. This is because the band in which the thermal emission peaks

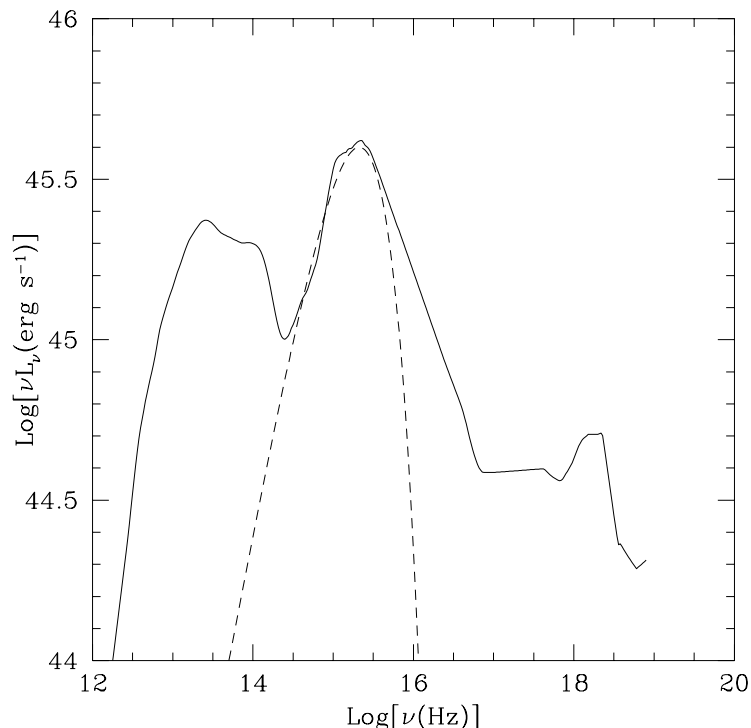


FIGURE 1. This failure of standard accretion disk models is especially prominent in AGN. Here the composite spectrum of radio-quiet quasars assembled by Elvis *et al.* (1994) is shown by the solid line, while a spectrum with the shape of equation 1.2 for $T_* = 7 \times 10^4$ K is shown by the dashed line.

for Galactic black holes (< 1 keV) is one for which, at least hitherto, spectroscopy has been relatively undeveloped, while in the ultraviolet, where the thermal component of AGN emission peaks, good quality spectroscopy is relatively easy to obtain. As Figure 1 shows, while the UV portion of the spectrum is, to zeroth order, replicated by the simple sum-of-blackbodies spectrum, our simple models of accretion disks don't come close to predicting the extremely broad-band emission seen in these objects.

2. Issues in Detailed Modelling

Given this much success, the next question to ask is whether more detailed predictions are equally successful. However, to make these predictions, we must first take a closer look at the accretion disk model under consideration. In particular, it contains at least two glaring omissions: we have ignored all relativistic corrections, yet by definition most of the light comes from a region whose gravitational potential is relativistically deep; and we have no assurance that the locally radiated spectrum is Planckian.

First consider the latter question. To answer it, we must solve three separate problems: the equilibrium radial structure of the disk (to find the optical depth as a function of radius); the equilibrium vertical structure (to find the temperature and density as a function of altitude at each radius); and the radiation transfer problem (to find the local emergent spectrum as a function of viewing angle). Unfortunately, there are major gaps in our understanding in each of these three areas. As a result, in each of them it is

necessary to make some unjustified assumption in order to proceed. Consequently, *every* detailed prediction of accretion disk spectra is model-dependent in important ways.

2.1. Radial structure

The fundamental equation governing the radial equilibrium is conservation of angular momentum:

$$- \int dz T_{r\phi} = \frac{\dot{M}\Omega}{2\pi} R_T(r) \quad (2.3)$$

$$= \frac{2\mu_e c^2}{e\sigma_T} \frac{\dot{m}}{x^{3/2}} R_T, \quad (2.4)$$

where $T_{r\phi}$ is the $r-\phi$ component of the stress tensor, \dot{M} is the mass accretion rate, Ω the local orbital frequency, and $R_T(r)$ is a correction factor which accounts for both relativistic effects and the outward transport of angular momentum [Novikov & Thorne (1973)]. The dimensionless form given in the second line is often the more useful one. In it, μ_e is the mass per electron, e is the radiative efficiency of accretion in rest-mass units, σ_T is the Thomson cross section, and x is the radius in gravitational units (*i.e.*, the unit of length is GM/c^2).

We do not yet know how to make a calculation from first principles for $T_{r\phi}$ in terms of other disk quantities. Instead, it has long been popular to appeal to dimensional analysis and guess that $T_{r\phi} = \alpha p$, where α is a dimensionless constant and p is the local pressure (Shakura & Sunyaev 1973). Recent simulations of the nonlinear development of magneto-rotational instabilities (Stone *et al.* 1996; Brandenburg *et al.* 1996; Brandenburg, this volume) suggest that this may, in fact, not be a bad approximation, and that $\alpha \sim 0.01 - 0.1$, but numerous uncertainties still remain. For example, it is not entirely clear *which* pressure sets the scale of the stress: gas pressure, radiation pressure, or magnetic pressure? Once this decision has been made, an equilibrium may be found if one assumes steady-state accretion and a smooth, geometrically thin structure for the disk. Its surface density is then $\propto \alpha^{-1}$, but it is also very sensitive to which pressure sets the scale. If the stress is proportional to the total pressure, the optical depth of the disk can be much smaller than if it scales with a pressure component that is only a fraction of the total. However, if $T_{r\phi}$ is proportional to the total pressure, when \dot{m} is more than a small fraction of unity, these equilibria are both viscously (Lightman & Eardley 1974) and thermally (Shakura & Sunyaev 1976) unstable. Does this mean that the “ α -prescription” breaks down at the level of perturbation theory? Or does it mean that some other equilibrium should be sought?

2.2. Vertical structure

Equally troubling questions arise when considering the details of vertical structure. The amount of local dissipation per unit area in an accretion disk is

$$Q = \frac{3}{4\pi} \frac{GM\dot{M}}{r^3} R_R(r) \quad (2.5)$$

$$= \frac{3\mu_e c^5}{GM\sigma_T e} \frac{\dot{m}}{x^3} R_R, \quad (2.6)$$

where R_R is a correction factor that accounts for both relativistic effects, and the outward transport of energy associated with the angular momentum flux [also worked out in Novikov & Thorne (1973)]. However, we do not know how this dissipation is distributed with height. Clearly, the run of temperature with altitude will be quite sensitive to the dissipation distribution.

In addition, when radiation pressure contributes significantly to the vertical support of the disk against gravity (as commonly occurs), there can be dramatic differences in

structure depending on where the radiation is created. For example, if all the dissipation takes place in the mid-plane, the radiation flux is constant with height, so that the vertical radiation force is simply proportional to the local opacity. On the other hand, if the dissipation is confined to the disk surface, there is no outward radiation flux in the body of the disk, and zero support against gravity. Moreover, if the dissipation takes place mostly within a few optical depths of the surface, its exact distribution will clearly have a major impact on the nature of the emergent radiation.

When radiation pressure dominates the vertical support, even small irregularities in the dissipation distribution can significantly affect the outgoing spectrum. Suppose, for example, that the dissipation in the body of the disk is proportional to the gas density. Then, because the flux increases linearly with altitude in exact balance with the increase of g_z with altitude, the effective vertical gravity is nil, and the density is constant as a function of height. However, at the very top of the disk this balance must be broken, for the density must fall to zero. The details of how sharply the density drops are very sensitive to exactly where the dissipation occurs because the effective gravity within the atmosphere depends on the balance between the small additional gravity gained by a small rise in altitude and the small additional radiation force due to the dissipation within that layer. These details are important because the photosphere generally lies within this region of the density roll-off.

The issue of how the heat deposition varies from place to place becomes still further confused when we consider the evidence that a significant part of the total emission comes out in hard X-rays, a portion of which may then shine down on the disk. In both AGN and Galactic black hole systems, there are telltale signs of X-ray illumination in the form of the ‘‘Compton reflection bump’’: Soft X-rays shining on cool material suffer strong photoelectric absorption, so the albedo of any accretion disk to photons from 0.5 – 10 keV is generally quite small, unless it is very thoroughly ionized. On the other hand, somewhat harder X-rays ($\sim 10 - 50$ keV) are very readily reflected by electron scattering because the highest energy photoionization edge of any abundant element is that of Fe at 7.1 keV, and photoionization cross sections drop rapidly with increasing energy above the edge. The reflection bump rolls over above 50 keV because higher energy photons lose energy by Compton recoil as they are reflected. These bumps are often so prominent that the corollary absorption must contribute significantly to disk heating.

This external illumination may substantially alter both the radial dependence of the integrated heating rate and the vertical distribution of heating at a fixed radius. Where it is important, the heating is largely confined to a skin whose thickness is at most a few Compton depths (*i.e.* $\sim 10^{24}$ cm $^{-2}$). Precisely because the energy is absorbed in such a thin layer, its effect there can be very strong. Because the photosphere frequently lies at a comparable depth from the surface, X-ray heating can have a major impact on features in the emergent spectrum.

In the limit that *most* of the heating occurs near the surface, whether due to segregation of the internal dissipation or external illumination, the instabilities endemic to radiation pressure-supported disks are quenched (Svensson & Zdziarski 1994). The reason is that there is then little outgoing radiation flux within the body of the disk, so it collapses to a state of substantially greater density (and also greater total surface density). Increases in the dissipation rate then have no impact on the thickness of the disk, and the feedback which drives the instabilities disappears.

2.3. Radiation transfer

While the transfer problem is entirely understood in principle, in practise it is so complicated that in every treatment so far, major approximations have been made. Thus,

for technical, rather than conceptual, reasons, the solutions are all, in one way or another, model-dependent. A major part of the art of constructing a good transfer solution therefore lies in adroit choices of approximations.

Certain features must surely be included in any transfer solution. Thomson opacity, for example, is almost always important. Similarly, it is easy to show that free-free opacity always affects at least the lower frequencies. At AGN temperatures, HI and HeII photoionization opacity are certainly significant, but at the higher temperatures of disks around stellar black holes, H and He are equally surely fully stripped.

Beyond this point, however, different workers have made different choices, and some effects may be important in certain ranges of parameter space, but not in others. For example, when computing the H and He photoionization opacity, it is necessary to make some statement about the ionization balance for these elements. The simplest guess is that the ionization fractions are those given by the Saha equation, but it is not obvious that this is always correct. Indeed, one might expect that the intensity of radiation in the H and HeII ionization continua would *couple* to the fractional ionization of these species. If one does wish to compute the actual ionization balance of H and He, there are further choices to be made about which processes are important and which are negligible. Ionizations can take place from excited states as well as the ground state, so the excited state population balance must also be found. How many states must be included? And which processes? In the most recent such calculation (Hubeny & Hubeny 1997), the H atom was permitted 9 different values of the principal quantum number, but all states having the same principal quantum number were assumed to be in detailed balance. In addition (and probably more significantly), only bound-free processes were considered. This may have been a significant oversight because at the densities prevalent in their disk model, the bound-bound transition rates due to electron collisions can be comparable to the bound-free rates. Moreover, because non-LTE effects are very sensitive to density, their character can depend very strongly on the model choices made when calculating the vertical structure of the atmosphere.

Another open question is the possible role of heavy element opacities. In AGN accretion disks, where the temperature might be $\sim 10^5$ K and the density $\sim 10^{14}$ cm $^{-3}$, the thermal equilibrium H neutral fraction is extremely small, $\sim 10^{-8}$. Partially-ionized stages of the more abundant heavy elements are therefore much *more* common than neutral H; the issue is whether the energy bands in which they have substantial opacity are important to the energy flow. Their ionization continua lie at relatively high energy (at least several tens of eV); their resonance lines have rather lower energy, but the importance of lines depends very strongly on the amplitude of turbulent motions in the disk. This last matter is, of course, central to the uncertainties already discussed regarding shear stress. In disks around stellar black holes, the Saha equation predicts that the dominant ionization stages will have ionization potentials $5 - 10kT$; however, there may be enough representatives of species with ionization potentials factors of a few smaller to significantly contribute to the opacity. This issue, too, also has implications for vertical structure when radiation pressure is an important part of the disk's vertical support.

A further question has to do with the possible effects of Comptonization. Its importance is gauged by the parameter

$$y \equiv (4kT/m_e c^2) \max(\tau_T, \tau_T^2), \quad (2.7)$$

for Compton optical depth τ_T . Here the relevant Compton depth is only that portion of the optical depth above the effective photosphere. When y is at least order unity, repeated Compton scatters may impart significant additional energy to photons before they leave the atmosphere. The magnitude of Comptonization is extremely sensitive to

model choices and parameters. For example, if the disk equilibrium is one in which the stress is proportional to the total pressure, the temperature in the atmosphere is close to the effective temperature, free-free absorption is the only absorptive opacity, and the gas pressure scale height in the atmosphere is comparable to the total disk thickness (an assumption likely to overestimate the importance of Comptonization),

$$y \simeq 0.6 \dot{m}^{5/3} m^{-1/6} \left(\frac{x}{10} \right)^{-5/2} R_R^{3/2} R_z^{-2/3} \frac{\omega^2}{(1 - e^{-\omega})^{2/3}}. \quad (2.8)$$

Here $\omega = h\nu/kT$, and R_z is another relativistic correction factor, this one adjusting the vertical component of the gravity (Abramowicz *et al.* 1997). The frequency-dependence of y is a consequence of the frequency-dependence of the effective photosphere's location. Unfortunately, at the present state of the art, Comptonization can only be treated within the diffusion equation for radiation transfer. Consequently, studies of Comptonization cannot also deal with questions involving either the angular distribution of the emergent radiation or sharp spectral features such as lines and edges. The second limitation comes about because these features are created by changes in the source function on scales comparable to a scattering length; hence, the diffusion approximation does not give an adequate description.

2.4. Relativistic effects

A final element that must be included in any proper model (but which is sometimes forgotten) is a proper accounting for relativistic effects. In addition to the dynamical corrections (encapsulated in R_R , R_T , and R_z), there are also relativistic photon propagation effects [Cunningham (1975)]. Disk material close to a black hole moves at speeds close to c ; as seen by a distant observer, its radiation is therefore Doppler boosted and beamed. In addition, there are intrinsically general relativistic effects: gravitational redshift, and photon trajectory bending. The last effect must be properly melded with the intrinsic angular radiation pattern of disk material in its own rest frame. Clearly, when (as will certainly happen here), Doppler shifts of order unity occur, there can be a dramatic impact on sharp spectral features such as lines and edges.

3. Results to Date

There have been many efforts over the past fifteen years or more to compute the spectra to be expected from accretion disks around black holes. The methods used include:

- stitching together stellar atmosphere solutions (Kolykhalov & Sunyaev 1984);
- summing local blackbodies, but applying general relativistic photon propagation effects (Sun & Malkan 1989);
- solving the frequency-dependent transfer problem, but assuming that the atmosphere is scattering-dominated at all locations and at all frequencies (Laor & Netzer 1989);
- solving the frequency-dependent transfer problem including non-LTE effects in H and He, but with non-standard stress prescriptions (Störzer *et al.* 1994, Hubeny & Hubeny 1997);
- solving the frequency-dependent transfer problem in LTE, but studying the effects of various stress prescriptions (Sincell & Krolik 1998) or external illumination (Sincell & Krolik 1997);
- solving the diffusion/Kompaneets equations in order to study Comptonization (Ross, Fabian & Mineshige 1992; Shimura & Takahara 1993; Dörrer *et al.* 1996).

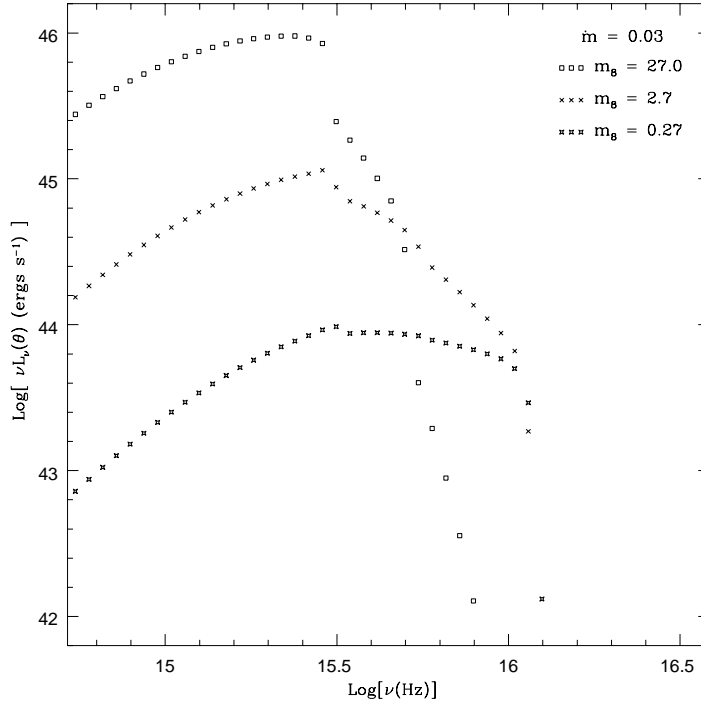


FIGURE 2. The predicted spectra from accretion disks around non-rotating supermassive black holes viewed pole-on. In all three cases shown, $\dot{m} = 0.03$, but the mass varies from $m = 3 \times 10^7$ to $m = 3 \times 10^9$ (from Sincell & Krolik 1998).

Because no one calculation is the most nearly complete, I will try to display the range of possibilities by showing a variety of calculations, each highlighting a different aspect of the problem. To set the stage, it's best to begin with how “standard” models depend on parameters. Figure 2 shows the scaling with central mass at fixed accretion rate relative to Eddington according to a calculation which employed full transfer solutions and general relativistic effects, but made the LTE approximation for the H and He ionization balances, and ignored all heavier elements. Although the luminosity increases in proportion to mass at fixed \dot{m} , the radiating area increases faster, $\propto m^2$. That is to say, the temperature at the innermost ring scales $\propto (\dot{m}/m)^{1/4}$. Consequently, as this quantity falls, the spectrum becomes softer and the Lyman edge goes steadily deeper and deeper into absorption. If, on the other hand, the central mass is held constant and the accretion rate is varied (Figure 3), the temperature rises, so increasing accretion rate both hardens the overall spectrum and throws the Lyman edge from absorption into emission. In the hottest disks, there can be substantial flux in the HeII continuum, although the edge itself generally stays in absorption for parameters appropriate to AGN.

3.1. *Dependence on radial structure model*

With this background, we may now inquire into the effects of the systematic uncertainties discussed in the previous section. First, how serious are the effects of the uncertainty in the radial equilibrium? Figure 4 shows what happens when the stress prescription is changed from αp_g to $\alpha \sqrt{p_g p_r}$ to $\alpha(p_r + p_g)$. Greater stress at fixed accretion rate leads to both smaller surface density and smaller volume density. Here the accretion rate is

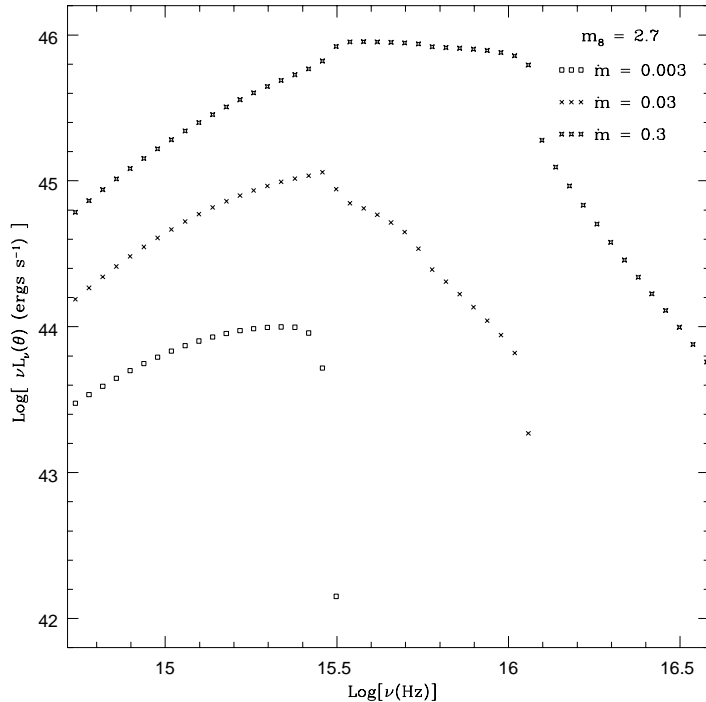


FIGURE 3. The predicted spectra from accretion disks around non-rotating supermassive black holes viewed pole-on. In all three cases shown, $m = 3 \times 10^8$, but the scaled accretion rate varies from $\dot{m} = 0.003$ to $\dot{m} = 0.3$ (from Sincell & Krolik 1998).

high enough that $p_r \gg p_g$ in the interesting inner rings of the disk. As a result, the temperature in the atmosphere is lowest in the αp_g case and highest when the stress is $\alpha(p_r + p_g)$. At fixed total luminosity, this leads to a generally harder overall spectrum for the disk with the greatest stress, but the qualitative character of the spectrum changes relatively little with different choices for the stress prescription.

3.2. Dependence on vertical distribution of heating

The next question to consider is the impact of the vertical distribution of heat deposition. In the most extreme limit, one in which all the heating is concentrated into the disk atmosphere (as, for example, X-ray heating may accomplish), the effects are dramatic. Because radiation pressure no longer supports the disk against the vertical component of gravity g_z , it is geometrically much thinner. Closer to the disk midplane, g_z is also smaller, so the gas pressure scale height (at fixed temperature) is longer. The density at the photosphere is then smaller, even though the density deep inside the disk is much greater. In addition, because the heating rate per unit mass rises upward in the X-ray-heated zone, so does the temperature (although not necessarily monotonically). The result is emergent spectra that are *softer* than the corresponding spectra from internally heated disks at low frequencies, but with more flux at higher frequencies, and ionization edges that are almost always in emission (compare Figure 5 to Figure 2).

FIGURE 4. The predicted spectrum from an accretion disk around a non-rotating supermassive black hole viewed pole-on. Here $\dot{m} = 0.3$ and $m = 3 \times 10^8$ (from Sincell & Krolik 1998).

3.3. Implications of the LTE approximation

Different approximations in the radiation transfer solution are the next issue whose effect we need to evaluate. Is it necessary (or when is it necessary) to compute the departure from LTE of the H and He ionization balances? Störzer *et al.* 1994 argued that when the photospheric pressure was > 100 dyne cm^{-2} (*i.e.*, the density $n \sim 10^{13} T_5^{-1} \text{ cm}^{-3}$), non-LTE effects are weak. However, Hubeny & Hubeny (1997) found that the LTE approximation seriously misrepresented the strength of the HI and HeII edges even when the photospheric pressure was several orders of magnitude greater. Part of the problem may be the definition of a non-LTE calculation: Hubeny & Hubeny (1997) included no bound-bound transitions in their evaluation of the H and He excited state balances. Another part of the problem (as already discussed in §2.2) may be that the character of the non-LTE effects is exquisitely sensitive to approximations in the solution of the hydrostatic equilibrium [an issue which affects both Störzer *et al.* 1994 and Hubeny & Hubeny (1997)]. Figure 6 illustrates what the effects of non-LTE *might* be. In this case, both the radiative acceleration and g_z were taken to be constant in the atmosphere, 9 bound levels of HI, 8 of HeI, and 14 of HeII were included, and all bound-bound transitions were neglected. Although the overall shape of the continuum is not very sensitive to non-LTE effects, they can completely change the nature of features at ionization edges.

3.4. Influence of heavy element opacity

Particularly in AGN accretion disks, heavy elements may potentially contribute substantially to the opacity, but these effects have just begun to be explored. To date there has been no calculation of how this added opacity may affect the vertical structure of the

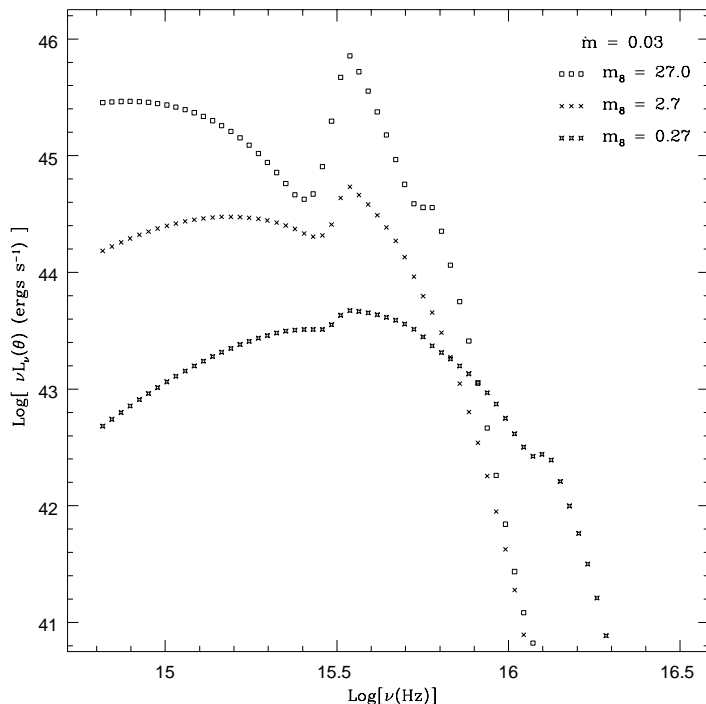


FIGURE 5. The predicted spectra from X-ray-illuminated accretion disks around non-rotating supermassive black holes viewed pole-on. In all three cases shown, $\dot{m} = 0.03$, but the mass varies from $m = 3 \times 10^7$ to $m = 3 \times 10^9$ (from Sincell & Krolik 1997).

disk, and therefore g_z in the atmosphere. Indeed, because including all the necessary atomic data is such a big job, and because the additional frequency resolution required to follow the multitude of heavy element lines adds such a large computational burden, there have been only partial calculations of these effects even assuming a vertical structure computed allowing only for H and He. For this reason, the spectrum shown in Figure 7 [Hubeny, Agol & Blaes (1998)] should be regarded merely as a demonstration of the potential impact of heavy element opacity. It was computed on the basis of an atmosphere solution whose vertical structure and temperature profile were determined including only H and He. Moreover, only those heavy element lines falling between 600\AA and 1400\AA were used. Nonetheless, the effects are large: the integrated outgoing flux is reduced by roughly a factor of two. An atmosphere which includes heavy element opacities in a fully self-consistent fashion will clearly look quite different from one with only H and He.

3.5. Impact of relativistic effects

As discussed in §2.4, there are two separate classes of relativistic effects: those entering the structural equations, and those affecting the appearance of the disk to distant observers. Both sorts of corrections are relatively modest when the black hole has little spin because the marginally stable orbit, at $x = 6$, is relatively far from the event horizon (at $x = 2$). However, as the spin increases, both the marginally stable orbit and the event horizon move inward, both approaching $x = 1$ as the spin increases toward its maximum value. Figure 8 shows how dramatic these effects can be. All three predicted spectra

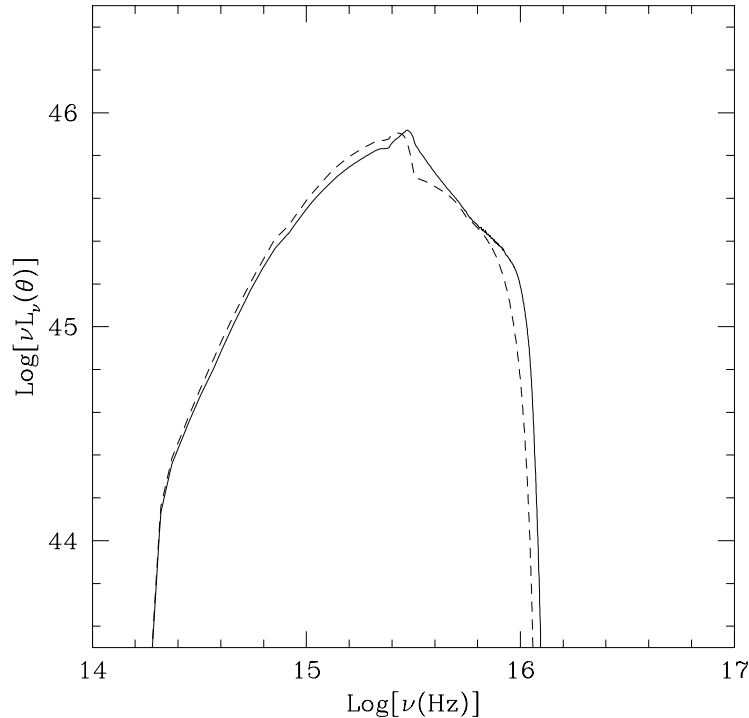


FIGURE 6. LTE (dashed line) and non-LTE (solid line) spectra from accretion disks around supermassive black holes viewed pole-on. In these calculations (Agol 1997), $\dot{m} = 0.072$ and $m = 2 \times 10^9$, and the normalized spin was 0.998.

were calculated using the same physics (stress proportional to $\sqrt{p_r p_g}$, LTE ionization fractions, no heavy elements) and pertain to the same m , \dot{m} , and viewing angle. When the central black hole spins rapidly, sharp edge features (as could be seen in the predictions for the spinless black hole) get stretched out over substantial frequency ranges. The HeII edge is stretched even farther than the HI edge because its origin is confined more nearly to the innermost radii. However, because the strongest relativistic effect is the Doppler boosting and beaming of radiation into the direction of orbital motion, these smoothing effects weaken considerably, even for rapidly-spinning black holes, when the viewing angle is nearly along the rotation axis.

4. Comparison to observations

Now that we have seen the range of spectral shapes predicted by various models, we can look at genuine observed spectra to see if any of their features are predicted by the models. Remarkably, the simplest approximation—summing local blackbodies without regard for any of the detailed physics we have discussed—does the best job of reproducing the observations! As shown in Figure 9, its slope comes very close to matching the composite slope (at least for the LBQS sample) at low frequencies, and, of course, it is absolutely clean at all ionization edges, in excellent agreement with the numerous observations showing that the Lyman edge is unobservably weak in the great majority of quasars [Koratkar, Kinney & Bohlin (1992)]. The zeroth-order approximation still fails, however, to explain the strength of the EUV continuum.

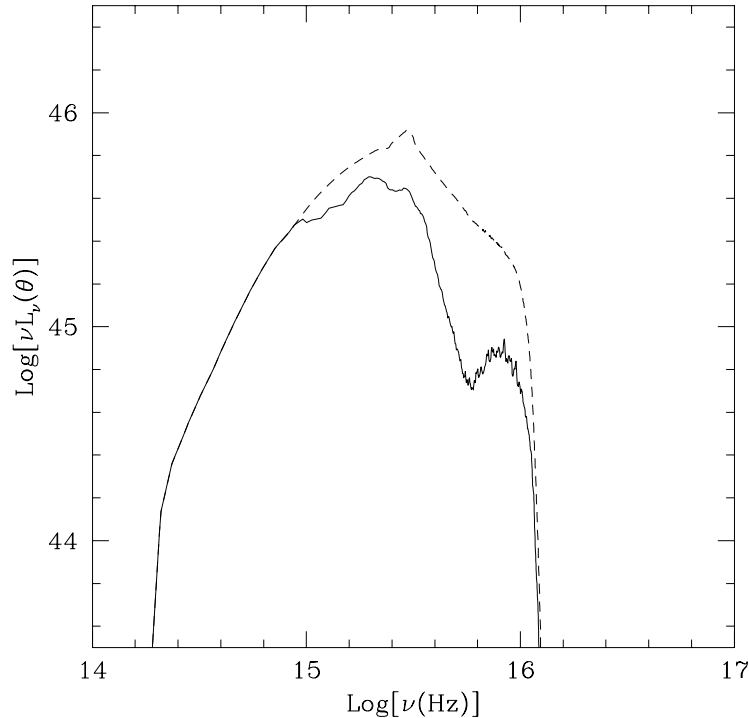


FIGURE 7. Effects of heavy element opacity on the spectrum from an accretion disk around a black hole with the same parameters as in Figure 6. As described in the text, the dashed line is a self-consistent disk spectrum whose opacity tables included only H and He; the solid line was calculated using the disk structure and temperature profile of the pure H and He model, but for predicting the outgoing flux, metal features between 600\AA and 1400\AA were included. The heavy element ionization fractions were assumed to be in LTE.

By contrast, the more detailed spectral predictions must be tuned to match the low frequency spectral shape, and nearly always show Lyman edge features, whether in emission or absorption. While it is possible to smooth out the edge with relativistic effects, it seems unlikely that the feature can disappear altogether in composite spectra unless polar views are somehow forbidden.

It is possible that Comptonization can solve two problems—the strength of the EUV continuum and the absence of Lyman edges, but it faces tough prerequisites. As Laor *et al.* (1997) have shown, the slope of the EUV spectrum as seen at the highest frequencies observable in the ultraviolet is a good predictor of the soft X-ray continuum, suggesting that this component extends smoothly all the way across the unobservable EUV. If this is true (the interpolation in Figure 1 assumes this), a significant fraction of the total luminosity of AGN is emitted in the EUV. To make this segment of the spectrum by Comptonization therefore entails putting the same fraction of the total dissipation into the Comptonizing layer. At present there is no known physical mechanism that will do so.

Thus, the interim conclusion regarding how well our models of accretion disks fare vis-a-vis observations is one that is frustrating in several respects. On the one hand, there are several major conceptual issues we do not know how to settle that introduce large uncertainties into our predictions; on the other hand, none of the guesses made to

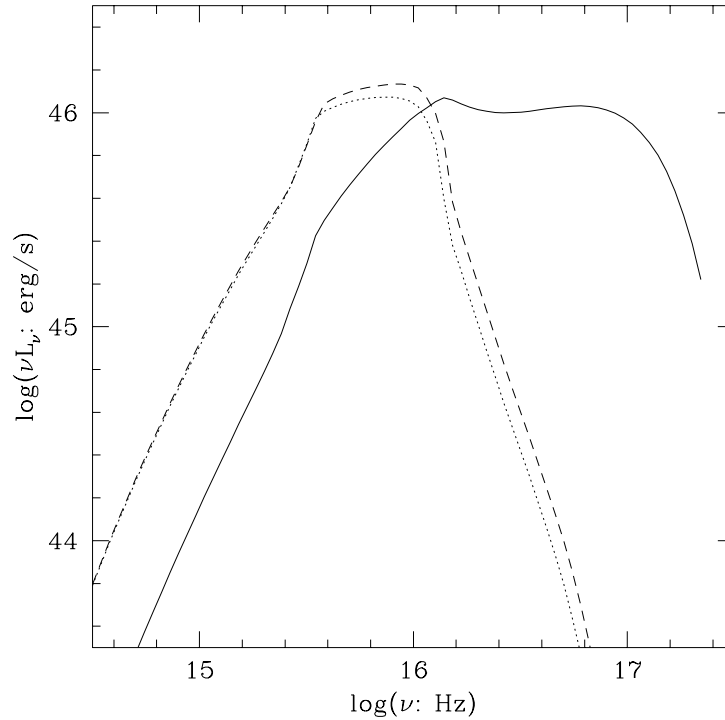


FIGURE 8. Effects of general relativity on the observed spectrum. All three curves are computed for a disk with $\dot{m} = 0.3$ around a black hole of mass $m = 3 \times 10^8$ viewed at an inclination angle of 40° . However, the dotted curve is the prediction of a model in which the black hole is spinless and the photons travel according to Newtonian rules, while the dashed curve shows how the same disk looks in the real, *i.e.*, relativistic world, and the solid curve shows the spectrum from the same disk if its central black hole had a normalized spin of 0.998.

date on how to resolve these questions leads to predictions that match observations. It seems quite likely that we are still missing a large piece of the puzzle.

I thank Eric Agol and Mark Sincell for many enlightening conversations, and for supplying figures, sometimes from unpublished work. My research on accretion disks is partially supported by NASA Grant NAG5-3929 and by NSF Grant AST-9616922.

REFERENCES

- AGOL, E. 1997 U. of California at Santa Barbara Ph.D. thesis
 ABRAMOWICZ, M.A., LANZA, A. & PERCIVAL, M.J. 1997 *Ap. J.* **479**, 179
 BRANDENBURG, A., NORDLUND, A., STEIN, R.F., & TORKESSON, U. 1996 *Ap. J. Letts.* **458**, L45
 CUNNINGHAM, C.T. 1975, *Ap.J.* **202**, 788
 DÖRRER, T.H., RIFFERT, H., STAUBERT, R., & RUDER, H. 1996 *Astron. & Astrop.* **311**, 69
 ELVIS, M., WILKES, B.J., MCDOWELL, J.C., GREEN, R.F., BECHTOLD, J., WILLNER, S.P., OEY, M.S., POLOMSKI, E., & CUTRI, R. 1994 *Ap. J. Suppl.* **95**, 1
 FRANCIS, P.J., HEWETT, P.C., FOLTZ, C.B., CHAFFEE, F.H., & WEYMANN, R.J. 1991 *Ap.J.* **373**, 465
 HUBENY, I., AGOL, E. & BLAES, O. 1998 in preparation

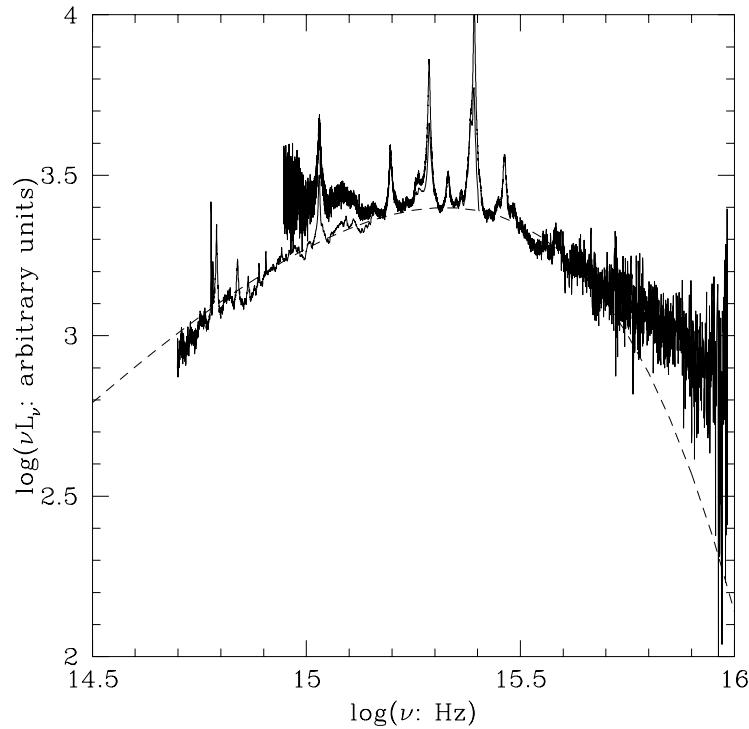


FIGURE 9. Match between a zeroth-order predicted disk spectrum and two composites of quasar spectra. The noisy solid curves are the composites assembled by Francis *et al.* (1991) (from the LBQS sample) and Zheng *et al.* (1997) (from the FOS archive); the dashed curve has the form $\nu^{4/3} \exp(-h\nu/kT)$ with $T = 7 \times 10^4$ K.

- HUBENY, I. & HUBENY, V. 1997 *Ap. J. Letts.* **484**, L37
 KORATKAR, A.P., KINNEY, A.L. & BOHLIN, R.C. 1992 *Ap.J.* **400**, 435
 LAOR, A., FIORE, F., ELVIS, M., WILKES, B.J. & MCDOWELL, J.C. 1997 *Ap.J.* **477**, 93
 LIGHTMAN, A.P. & EADLEY, D.M. 1974 *Ap. J. Letts.* **187**, L1
 NOVIKOV, I.D. & THORNE, K.S. 1973 In *Black Holes* (eds. C. De Witt & B. De Witt), p. 343. Gordon and Breach.
 RFM92] ROSS, R.R., FABIAN, A.C. & MINESHIGE, S. 1992 *M.N.R.A.S.* **258**, 189
 SHAKURA, N.I. & SUNYAEV, R.A. 1973 *Astron. & Astrop.* **24**, 337
 SHAKURA, N.I. & SUNYAEV, R.A. 1976 *M.N.R.A.S.* **175**, 613
 SHIMURA, T. & TAKAHARA, F. 1993 *Ap. J.* **419**, 78
 SINCELL, M.W. & KROLIK, J.H. 1997 *Ap. J.* **476**, 605
 SINCELL, M.W. & KROLIK, J.H. 1998 *Ap. J.* in press
 STONE, J.M., HAWLEY, J.F., GAMMIE, C.F., & BALBUS, S.A. 1996 *Ap. J.* **463**, 656
 STÖRZER, H., HAUSCHILDT, P.H., & ALLARD, F. 1994 *Ap. J. Letts.* **437**, L91
 SVENSSON, R. & ZDZIARSKI, A. 1994 *Ap. J.* **436**, 599
 ZHENG, W., KRIS, G.A., TELFER, R.C., GRIMES, J.P. & DAVIDSEN, A.F. 1997 *Ap.J.* **475**, 469